The Filtered-x Least Mean Fourth Algorithm for Active Noise Control and Its Convergence Analysis

*Kang Seung Lee and **Dae Hee Youn

Abstract

In this paper, we propose the filtered-x least mean fourth (LMF) algorithm where the error raised to the power of four is minimized and analyze its convergence behavior for a multiple sinusoidal acoustic noise and Gaussian measurement noise. Application of the filtered-x LMF adaptive filter to active noise control (ANC) requires estimating of the transfer characteristic of the acoustic path between the output and error signal of the adaptive controller. The results of the convergence analysis of the filtered-x LMF algorithm indicates that the effects of the parameter estimation inaccuracy on the convergence behavior of the algorithm are characterized by two distinct components: Phase estimation error and estimated gain. In particular, the convergence is shown to be strongly affected by the accuracy of the phase response estimate. Also, we newly show that convergence behavior can differ depending on the relative sizes of the Gaussian measurement noise and convergence constant.

Ⅰ. Introduction

In active noise control, the acoustic noise to be cancelled is often generated by rotating machines and thus can be modeled as the sum of a fundamental sinusoid and its harmonics. In this paper we are concerned with cancellation of fan noise based on ANC filtering. Fan noise is frequently generated in the consumer electronic products such as air conditioners, vacuum cleaners and so on. Adaptive approaches have widely been used in ANC applications in which the unwanted noise sound is adaptively synthesized with the equal amplitude but opposite phase, resulting in the cancellation of the acoustic noise as shown in Fig. 1[1][2]. In Fig. 1, the input microphone can be replaced by other non-acoustical sensors such as tachometers or accelerometers in which case the possibility of the speaker output feedback to the input microphone is removed. The adaptive filter output drives the loudspeaker in such a way that the acoustic noise and the loudspeaker output can be summed to null at the error microphone.

Although any adaptive algorithm can be used in Fig. 1, the least mean square (LMS) algorithm has been the most popular one[3][4]. It has recently been found that the LMF algorithm in which the error raised to the power of four is minimized has better convergence properties[5]. It is noted, however, that the direct application of the LMS algorithm in Fig. 1 is not appropriate. The reason is that the acoustic path between the filter output and summation point of the error signal is frequency sensitive, which acts to distort the phase and magnitude of the error signal. In turn, the distortion of the phase and magnitude in the error path can degrade the convergence performance of the LMS algorithm. As a result, the convergence rate is lowered, the residual error is increased, and the algorithm can even become unstable. For these reasons, it is necessary to use the so-called Filtered-x LMS algorithm[6] for which the transfer characteristics between the output and the error signal of the adaptive controller must be estimated.

In this paper, we propose a new filtered-x LMF algorithm for active cancellation of fan noise. It is noted that the fan noise can be modeled as the sum of a fundamental sinusoid and its harmonics. We first derive an adaptive canceller structure and then analyze its convergence behavior when the acoustic noise can be modeled as the sum of a fundamental sinusoid and its harmonics. The convergence analysis is focused on the effects of parameter estimation inaccuracy on the performance.

Ⅱ. ANC System Model and Algorithm

Since the loudspeaker-air-microphone path of Fig. 1 is

*Department of Computer Engineering, Dongeui University
**Department of Electronic Engineering, Yonsei University
Manuscript Received July 29, 1996.

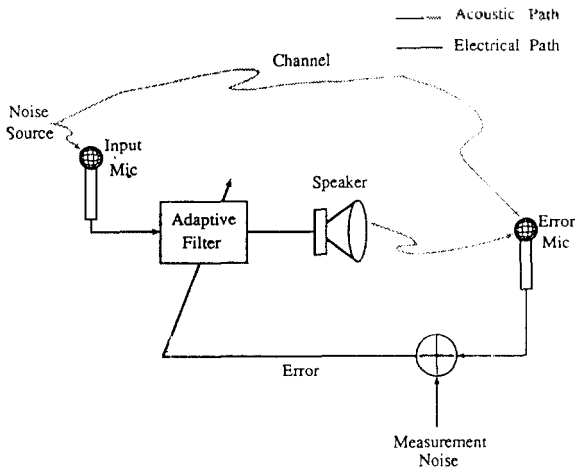

Figure 1. Basic adaptive active noise controller configuration.

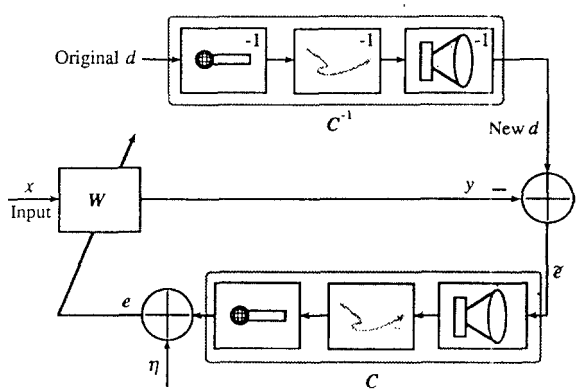

Figure 2. Rearranged form of the controller under linear system condition.

linear, one can easily get the equivalent system as shown in Fig. 2. When the noise consists of the multiple sinusoids, which is the case of fan noise, the acoustic and loud-speaker-acoustic-microphone can be described by the multiple in-phase (I) and quadrature (Q) weights as shown in the upper branch of Fig. 3.

For the m-th sinusoidal noise, the adaptive canceller structure also becomes to have two weights $\omega_{I,m}(n)$ and $\omega_{Q,m}(n)$, with I and Q inputs, $x_{I,m}(n)$ and $x_{Q,m}(n)$, respectively. Thus the output of the m-th controller, $y_m(n)$ is expressed as

$$y_m(n) = \{w_{I,m}(n)\, x_{I,m}(n) + x_{Q,m}(n)\, w_{Q,m}(n)\} \tag{1}$$

where

$$x_{I,m}(n) = A_m \cos(\omega_m n + \phi_m) \triangleq A_m \cos \Psi_m(n),$$
$$x_{Q,m}(n) = A_m \sin(\omega_m n + \phi_m) \triangleq A_m \sin \Psi_m(n),$$

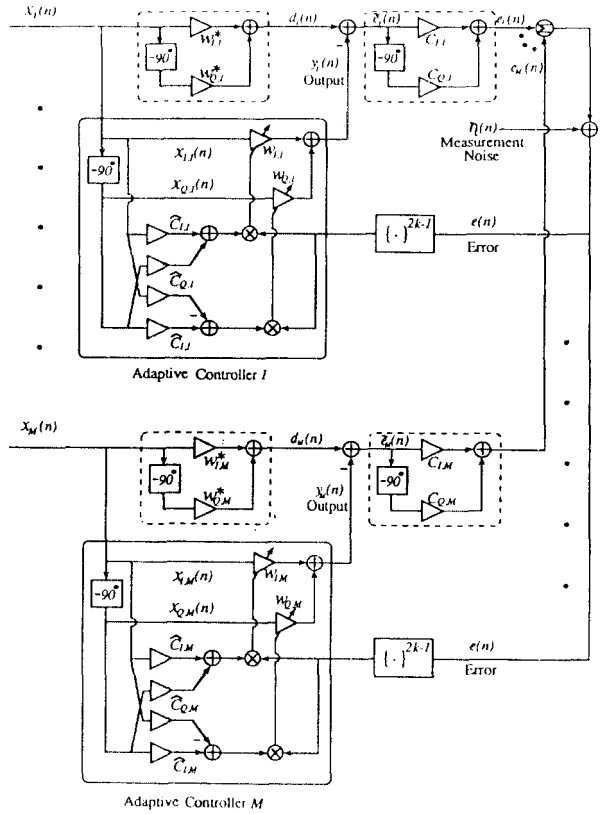

Figure 3. The diagram of adaptive active noise controller system under study.

m: branch index = 1, 2, 3,..., M,
n: discrete time index,
A: amplitude,
ω: normalized frequency,
Ψ: random phase.

Also, referring to the notation in Fig. 3, the error signal $e(n)$ is represented by

$$\begin{aligned} e(n) &= \sum_{m=1}^{M} [c_{I,m}\, \tilde{e}_{I,m}(n) + c_{Q,m}\, \tilde{e}_{Q,m}(n)] + \eta(n) \\ &= -\sum_{m=1}^{M} A_m [c_{I,m} \cos \Psi_m(n) + c_{Q,m} \sin \Psi_m(n)]\, \{w_{I,m}(n) - w_{I,m}^*\} \\ &\quad - \sum_{m=1}^{M} A_m [c_{I,m} \sin \Psi_m(n) - c_{Q,m} \cos \Psi_m(n)]\, \{w_{Q,m}(n) - w_{Q,m}^*\} \\ &\quad + \eta(n) \end{aligned} \tag{2}$$

where

$$\tilde{e}_I(n) \triangleq \tilde{e}(n) = \sum_{m=1}^{M} \{d_m(n) - y_m(n)\},$$

$\tilde{e}_Q(n)$: 90° phase-shifted version of $\tilde{e}_I(n)$
$\eta(n)$: zero-mean measurement noise.

Assuming that $\omega_{I,m}(n)$ and $\omega_{Q,m}(n)$ are slowly time-varying as compared to $x\omega_{I,m}(n)$ and $x_{Q,m}(n)$, the phase-shifted output is giver from (1) by

$$y_Q(n)=\sum_{m=1}^{M}\{w_{I,m}(n)\,x_{Q,m}(n)-w_{Q,m}(n)\,x_{I,m}(n)\}$$
$$=\sum_{m=1}^{M}A_m\{w_{I,m}(n)\sin\Psi_m(n)-w_{Q,m}(n)\cos\Psi_m(n)\}. \quad (3)$$

It can be shown from (1), (2) and (3) that minimizing the fourth power error and using a gradient-descent method yields [3] a pair of the filtered-x LMF weight update equations for each m as

$$w_{I,m}(n+1)=w_{I,m}(n)+\mu_m k^{2k-1}(n)\{c_{I,m}x_{I,m}(n)+c_{Q,m}x_{Q,m}(n)\},$$
$$w_{Q,m}(n+1)=w_{Q,m}(n)+\mu_m k^{2k-1}(n)\{c_{I,m}x_{Q,m}(n)-c_{Q,m}x_{I,m}(n)\}. \quad (4)$$

where $m=1, 2,\ldots, M$ and μ_m is a convergence constant.

It is noted that to implement the filtered-x LMF algorithm of (4), the values of $c_{I,m}$ and $c_{Q,m}$ must be estimated. In the following, we tanalyze the effects of replacing $c_{I,m}$ and $c_{Q,m}$ in (4) with $\hat{c}_{I,m}$ and $\hat{c}_{Q,m}$ on the convergence behavior of the canceller.

Ⅲ. Convergence Analysis

A. The mean of weight error(Magnitude)

To see how the adaptive algorithm derived in (4) converges for inaccurate $\hat{c}_{I,m}$ an $\hat{c}_{Q,m}$, we first investigate the convergence of the expected values of the adaptive weights. To simplify the convergence equation, we may introduce two weight errors as

$$v_{I,m}(n)\triangleq w_{I,m}(n)-w^*_{I,m},$$
$$v_{Q,m}(n)\triangleq w_{Q,m}(n)-w^*_{Q,m}. \quad (5)$$

Then, from (2), (5) and Fig. 3, we get

$$\tilde{e}_{I,m}(n)=-v_{I,m}(n)\,x_{I,m}(n)-v_{Q,m}(n)\,x_{Q,m}(n),$$
$$\tilde{e}_{Q,m}(n)=-v_{I,m}(n)\,x_{Q,m}(n)+v_{Q,m}(n)\,x_{I,m}(n). \quad (6)$$

Inserting (5) into (4), we have

$$v_{I,m}(n+1)=v_{I,m}(n)+2\mu_m e^3(n)\{\hat{c}_{I,m}x_{I,m}(n)+\hat{c}_{Q,m}x_{Q,m}(n)\},$$
$$v_{Q,m}(n+1)=v_{Q,m}(n)+2\mu_m e^3(n)\{\hat{c}_{I,m}x_{Q,m}(n)-\hat{c}_{Q,m}x_{I,m}(n)\}. \quad (7)$$

Rearranging (7) with (2) and (6), taking expectation of both sides of the resultant two weight-error equations, we can get the convergence equation based on the independent assumption on the underlying signal; $x_m(n)$, $\eta(n)$, $v_{I,m}$ and $v_{Q,m}$.

The Moment terms of order greater than 1 decrease much faster than the first order moment term in $E[v_{I,m}(n)]$ and $E[v_{Q,m}(n)]$. Therefore, ignoring the moment terms order greater than 1, the convergence equation becomes

$$\begin{bmatrix}E[v_{I,m}(n+1)]\\E[v_{Q,m}(n+1)]\end{bmatrix}\cong\begin{bmatrix}\alpha_m & \beta_m\\-\beta_m & \alpha_m\end{bmatrix}\begin{bmatrix}E[v_{I,m}(n)]\\E[v_{Q,m}(n)]\end{bmatrix} \quad (8)$$

where

$$\alpha_m\triangleq 1-3\mu_m A_m^2 g_m\hat{g}_m\sigma_\eta^2\cos\triangle\theta_{c,m},$$
$$\beta_m\triangleq 1-3\mu_m A_m^2 g_m\hat{g}_m\sigma_\eta^2\sin\triangle\theta_{c,m}.$$

Here, defining gain and phase response parameters as

$$g_m \triangleq\sqrt{c_{I,m}^2+c_{Q,m}^2},$$
$$\hat{g}_m \triangleq\sqrt{\hat{c}_{I,m}^2+\hat{c}_{Q,m}^2},$$
$$\theta_{c,m} \triangleq\tan^{-1}\left(\frac{c_{Q,m}}{c_{I,m}}\right),$$
$$\hat{\theta}_{c,m} \triangleq\tan^{-1}\left(\frac{\hat{c}_{Q,m}}{\hat{c}_{I,m}}\right),$$
$$\triangle\theta_{c,m}\triangleq\theta_{c,m}-\hat{\theta}_{c,m}.$$

Now, using the similarity transform to make $E[v_{I,m}(n)]$ and $E[v_{Q,m}(n)]$ in decoupled forms, (8) can be expressed as follows.

$$\begin{bmatrix}E[\tilde{v}_{I,m}(n+1)]\\E[\tilde{v}_{Q,m}(n+1)]\end{bmatrix}=\begin{bmatrix}1-\lambda_{I,m} & 0\\0 & 1-\lambda_{Q,m}\end{bmatrix}\begin{bmatrix}E[\tilde{v}_{I,m}(n)]\\E[\tilde{v}_{Q,m}(n)]\end{bmatrix} \quad (9)$$

where

$$\lambda_{i,m}=3\mu_m A_m^2 g_m\hat{g}_m\sigma_\eta^2[\cos\triangle\theta_{c,m}\pm j\sin\triangle\theta_{c,m}],\ i=I,Q.$$

Since $\lambda_{I,m}$ in (9) is a complex number, the transformed weight error is also complex. When a complex number is given, we consider its real and imaginary parts individually or investigate the convergence of magnitude of transformed weight error.

$$|E[v_{i,m}(n+1)]|=|1-\lambda_{i,m}||E[v_{i,m}(n)]|,\ i=I,Q. \quad (10)$$

As it is clearly seen in(10), the magnitude of weight error converges exponentially to 0 under following conditions.

$$|1-\lambda_{i,m}|<1 \quad \forall_{i,m}, \quad i=I,Q. \quad (11)$$

Squaring both sides of(11) and rearranging the terms, the stabilizing condition are obtained.

$$0 < \mu_m < \frac{2\cos\triangle\theta_{c,m}}{3A_m^2 g_m \hat{g}_m \sigma_\eta^2} \quad \text{or} \quad 0 < \chi_{m,f} < 1. \tag{12}$$

where

$$\chi_{m,f} \triangleq \frac{3\mu_m A_m^2 g_m \hat{g}_m \sigma_\eta^2}{2\cos\triangle\theta_{c,m}}.$$

We see that stabilizing condition of (12), unlike the filtered-x LMS, is affected by variance of measurement noise signal[7][8]. In a sufficiently large time constant τ domain, time constant τ for exponential convergence can be simplified and is derived[3].

$$e^{-1/\tau_{i,m}} \cong 1 - \frac{1}{\tau_{i,m}} = |1-\lambda_{i,m}|,\ i = I, Q. \tag{13}$$

From (10) and (13) the time constant is

$$\tau_i = \frac{1}{1-\sqrt{1-6\mu_m A_m^2 g_m \hat{g}_m \sigma_\eta^2 \cos\triangle\theta_{c,m} + 9\mu_m^2 A_m^4 g_m^2 \hat{g}_m^2 \sigma_\eta^4}},\quad i = I, Q$$

$$= \frac{1}{1-\sqrt{1-4\chi_{m,f}(1-\chi_{m,f})\cos^2\triangle\theta_{c,m}}}. \tag{14}$$

B. Summed variance of weight errors

Next we investigate the convergence of the mean-square error (MSE), $E[e^2(n)]$. Using (2) and (6), we can express the MSE as

$$E[e^2(n)] = \sum_{m=1}^{M} e_m^2(n) + \sigma_\eta^2 = \frac{1}{2}\sum_{m=1}^{M} A_m^2 \xi_m(n) + \sigma_\eta^2 \tag{15}$$

where

$$\xi_m(n) \triangleq E[v_{I,m}^2(n)] + E[v_{Q,m}^2(n)],$$
$$\sigma_\eta^2 \triangleq E[\eta^2]$$

From (15), we find that studying the convergence of MSE is directly related to studying the sum of $\xi_m(n)$. Inserting (1) and (2) into (5), and assuming that input signal $x_m(n)$, measure noise $\eta(n)$, and weight errors $v_{I,m}(n)$, $v_{Q,m}(n)$ are independent of each other, we take the statistical average of both sides to obtain two equations for $E[v_I^2(n+1)]$, $E[v_Q^2(n+1)]$. Since there two equations are symmetrical, we add them and assume that $E[v_I^2(n+1)] \cong E[v_Q^2(n+1)]$. Thus, eliminating the subscripts I and Q to simplify the second moment equation of weight error and rearranging the terms yields

$$\begin{aligned}
E[v_m^2(n+1)] &= \frac{5}{4}\mu_m^2 A_m^8 g_m^6 \hat{g}_m^2 \{E[v_m^6(n)] + 3E[v_m^2(n)]E[v_m^4(n)]\} \\
&\quad -\frac{3}{2}\mu_m A_m^4 g_m^3 \hat{g}_m \cos\triangle\theta_{c,m}\{E[v_m^4(n)] + (E[v_m^2(n)])^2\} \\
&\quad +\frac{45}{2}\mu_m^2 A_m^6 g_m^4 \hat{g}_m^2 E[\eta^2(n)]\{E[v_m^4(n)] + (E[v_m^2(n)])^2\} \\
&\quad +\{1-6\mu_m A_m^2 g_m \hat{g}_m E[\eta^2(n)]\cos\triangle\theta_{c,m} \\
&\quad +30\mu_m^2 A_m^4 g_m^2 \hat{g}_m^2 E[\eta^4(n)]\} E[v_m^2(n)] \\
&\quad +2\mu_m^2 A_m^2 \hat{g}_m^2 E[\eta^6(n)].
\end{aligned} \tag{16}$$

Assuming that $\eta(n)$ is a Gaussian with zero average and $v_{I,m}(n)$, $v_{Q,m}(n)$ are Gaussian variables, $v_m(n)$ is also a Gaussian variable. Thus, (16) can be simplified by expressing $E[v_m^{2K}(n)]$ as $E[v_m^2(n)]$ Although $E[v_m(n)]$ decreases very rapidly, it is no zero from the beginning. Thus, a Gaussian random variable $\triangle w_m(n)$ with zero average, and its variance are adapted as follows:

$$\triangle w_m(n) \triangleq v_m(n) - V_m(n),$$
$$E[v_m^2(n)] = V_m^2(n) + \rho_m^2(n) \tag{17}$$

where $V_m(n) \triangleq E[v_n(n)]$,
$\rho_m^2(n) \triangleq E[\triangle^2 w_m(n)]$.

From (17), we find that during the transient state, i.e. from beginning to the moment just before the steady state, $\rho_m^2(n)$ is much smaller than $V_m^2(n)$ and $E[v_m(n)]$ can be regarded as $V_m^2(n)$. On the other hand, $\rho_m^2(n)$ becomes dominant over $V_m^2(n)$ in the steady state and $E[v_m(n)]$ can be regarded as $\rho_m^2(n)$. Now, apply (17) to (16) and use the relationship between $E[v_m^{2K}(n)]$ and $E[v_m^2(n)]$ of the Gaussian random variable[9] to arrive at the following equation.

$$\begin{aligned}
V_m^2(n+1) + \rho_m^2(n+1) &= 5\mu_m^2 A_m^8 g_m^6 \hat{g}_m^2\{V_m^6(n) + 9\rho_m^2(n)V_m^4(n) + 18\rho_m^4(n)V_m^2(n) + 6\rho_m^6(n)\} \\
&\quad -(3\mu_m A_m^4 g_m^3 \hat{g}_m \cos\triangle\theta_{c,m} - 45\mu_m^2 A_m^6 g_m^4 \hat{g}_m^2 \sigma_\eta^2) \\
&\quad \{V_m^4(n) + 4\rho_m^2(n)V_m^2(n) + 2\rho_m^4(n)\} \\
&\quad +(1-6\mu_m A_m^2 g_m \hat{g}_m \sigma_\eta^2 \cos\triangle\theta_{c,m} + 90\mu_m^2 A_m^4 g_m^2 \hat{g}_m^2 \sigma_\eta^4) \\
&\quad \{V_m^2(n) + \rho_m^2(n)\} \\
&\quad +30\mu_m^2 A_m^2 \hat{g}_m^2 \sigma_\eta^6.
\end{aligned} \tag{18}$$

(1) Convergence during the transient state

The convergence equation (18) may be examined for two different cases, First, $\rho_m^{2K}(n)$ and the last term of (18) can be removed for the transient state. Thus, the transient convergence equation is given by

$$V_m^2(n+1) \cong 5\mu_m^2 A_m^8 g_m^6 \hat{g}_m^2 V_m^6(n) - (3\mu_m A_m^4 g_m^3 \hat{g}_m \cos\triangle\theta_{c,m} - 45\mu_m^2 A_m^6 g_m^4 \hat{g}_m^2 \sigma_\eta^2) V_m^4(n) + (1 - 6\mu_m A_m^2 g_m \hat{g}_m \sigma_\eta^2 \cos\triangle\theta_{c,m} + 90\mu_m^2 A_m^4 g_m^2 \hat{g}_m^2 \sigma_\eta^4) V_m^2(n). \quad (19)$$

On the right side of (19), either $V_m^6(n)$ or $V_m^2(n)$ becomes a dominant term in extreme cases. When the two terms have same values, we can write $V_m^2(n)$ as follow

$$V_{m,th}^2 = \frac{\sqrt{1 - 6\mu_m A_m^2 g_m \hat{g}_m \sigma_\eta^2 \cos\triangle\theta_{c,m} + 90\mu_m^2 A_m^4 g_m^2 \hat{g}_m^2 \sigma_\eta^4}}{5\mu_m^2 A_m^8 g_m^6 \hat{g}_m^2} \quad (20)$$

Note that $\triangle\theta_{c,m}$ does not affect $V_{m,th}^2$. In (19), the first term $V_m^6(n)$ acts as the dominant term when $V_m^2(n)$ is greater than $V_{m,th}^2$. If V_m^2 is smaller than $V_{m,th}^2$, then the last $V_m^6(n)$ term becomes dominant. Fig. 4 is given to illustrate in terms of the convergence constant μ_m and the variance of measurement noise σ_η^4, which of the two terms, the first term $V_m^6(n)$ and the last term $V_m^2(n)$, is dominant when $V_{m,th}^2(n) = 0.8$. Point (a) is a region in which the term $V_m^6(n)$ dominates over the other and point (b) is when $V_m^2(n)$ term is the dominant one. Therefore, the transient convergence equation (19) can be written as:

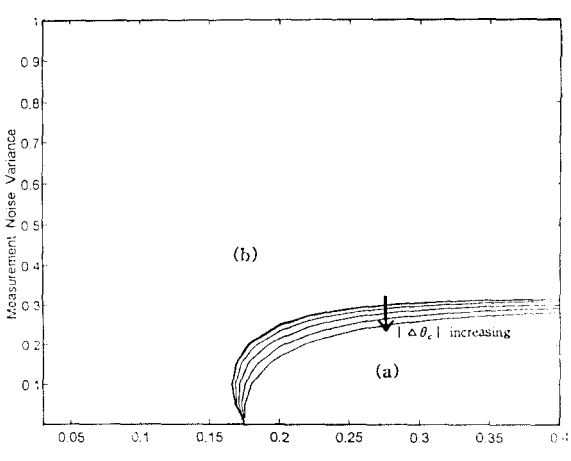

Figure 4. Dominant term decision diagram for filtered-x LMF algorithm of summed variance of weight errors at the transient-state.

$$V_m^2(n+1) \cong \begin{cases} 5\mu_m^2 A_m^8 g_m^6 \hat{g}_m^2 V_m^6(n), & V_m^2(n) \gg V_{m,th}^2 \quad (21a) \\ (1 - 6\mu_m A_m^2 g_m \hat{g}_m \sigma_\eta^2 \cos\triangle\theta_{c,m} + 90\mu_m^2 A_m^4 g_m^2 \hat{g}_m^2 \sigma_\eta^4) V_m^2(n), & V_m^2(n) \ll V_{m,th}^2. \quad (21b) \end{cases}$$

Now, from (21a) we may derive the conditions for stability and the time constant by rewriting it as

$$V_m^2(n) = \{5\mu_m^2 A_m^8 g_m^6 \hat{g}_m^2\}^{(3^n-1)/2} \{V_m^2(0)\}^{3^n} = \frac{1}{\sqrt{5}\mu_m A_m^4 g_m^3 \hat{g}_m} \{\sqrt{5}\mu_m A_m^4 g_m^3 \hat{g}_m V_m^2(0)\}^{3^n}. \quad (22)$$

Thus, (22) is stable under the following condition:

$$|\sqrt{5}\mu_m A_m^4 g_m^3 \hat{g}_m V_m^2(0)| < 1,$$

$$0 < \mu_m < \frac{1}{\sqrt{5} A_m^4 g_m^3 \hat{g}_m V_m^2(0)}. \quad (23)$$

Note from the conditions for stability in (23) that the initial value of weight error acts as a limiting factor, along with the amplitude of input signal, the gain of the secondary path and the estimated gain of the secondary path. And, (21b) is stabilized when it satisfies the condition below:

$$0 < \mu_m < \frac{\cos\triangle\theta_{c,m}}{15 A_m^2 g_m \hat{g}_m \sigma_\eta^2} \text{ or } 0 < \chi_{m,s} < 1 \quad (24)$$

where

$$\chi_{m,s} \triangleq \frac{15\mu_{FX,m} A_m^2 g_m \hat{g}_m \sigma_\eta^2}{\cos\triangle\theta_{c,m}}.$$

From (13) and (21b), the time constant is given by;

$$\tau_{m,s} = \frac{1}{6\mu_m A_m^2 g_m \hat{g}_m \sigma_\eta^2 \{\cos\triangle\theta_{c,m} - 15\mu_m A_m^2 g_m \hat{g}_m \sigma_\eta^2\}} = \frac{5}{2\chi_{m,s}\cos^2\triangle\theta_{c,m}\{1 - \chi_{m,s}\}}. \quad (25)$$

(2) Convergence in the steady state

In the steady state, $V_m^2(n)$ becomes sufficiently small and the terms that include $\rho_m^4(n)$ and $\rho_m^6(n)$ can be ignored in the convergence equation (18). The equation is then simplified as

$$\rho_m^2(n+1) \cong (1 - 6\mu_m A_m^2 g_m \hat{g}_m \sigma_\eta^2 \cos\triangle\theta_{c,m} + 90\mu_m^2 A_m^4 g_m^2 \hat{g}_m^2 \sigma_\eta^4) \rho_m^2(n)$$

$$+30\,\mu_m^2 A_m^2 g_m^2 \hat{g}_m^2 \sigma_\eta^6. \tag{26}$$

And, the summed variance of weight errors in the steady state, $\xi_m(\infty)$ is $2\,\rho_m(\infty)$ and it can be written as

$$\xi_m(\infty)=2\,\rho_m(\infty)=\frac{10\mu_m \hat{g}_m \sigma_\eta^4}{g_m\{\cos\triangle\theta_{c,m}-15\mu_m A_m^2 g_m \hat{g}_m \sigma_\eta^2\}}$$

$$=\frac{2\sigma_\eta^2 \chi_{m,s}}{3A_m^2 g_m^2\{1-\chi_{m,s}\}}. \tag{27}$$

(3) Comparison of the FXLMF and FXLMS algorithm

Comparing the performance of adaptive algorithms usually involves two methods. The first method is to compare the state of convergence after setting equal values for the steady state, and the other one involves comparing the steady state values for same rate of convergence.

Like (18) in [8] the summed variance of weight errors of the FXLMS algorithm is a geometric series and the time constant can be defined while that of the FXLMF algorithm (18) is not a geometric series and therefore, the time constant may not be defined. Then we set the steady state values of the two algorithms equal and compare the convergence rates. From (27) and (20) in [8] we obtain following equation.

$$\frac{10\mu_{Fx,m}\hat{g}_m\sigma_\eta^2}{g_m\{\cos\triangle\theta_{c,m}-15\mu_{Fx,m}A_m^2 g_m\hat{g}_m\sigma_\eta^2\}}$$

$$=\frac{\mu_{Sx,m}\hat{g}_m\sigma_\eta^2}{g_m\{\cos\triangle\theta_{c,m}-\frac{1}{16}\mu_{Sx,m}A_m^2 g_m\hat{g}_m(9-\cos 2\triangle\theta_{c,m})\}} \tag{28}$$

where $\mu_{Fx,m}$ and $\mu_{Sx,m}$ are the convergence constants of FXLMF and FXLMS algorithms, respectively.

When the convergence constants $\mu_{Fx,m}$ and $\mu_{Sx,m}$ satisfy the stability conditions, the second terms on both sides of (28) are sufficiently smaller than the first terms and they are ignored to yield the following equation.

$$\mu_{Fx,m}=\frac{\mu_{Sx,m}}{10\sigma_\eta^2}. \tag{29}$$

Ⅳ. Computer Simulation

In this section, we present the results obtained from computer simulation along with the theoretical analysis of FXLMF algorithm in the previous section.

case 1. the convergence property of FXLMF algorithm.

case 2. the performance comparison of FXLMF and FXLMS.

We set the frequencies of the first and second sinusoidal signal at 120 Hz and 240 Hz, respectively, and selected 2 KHz for sampling frequency. The input signal $x(n)$ and desired signal $d(n)$ are given by

$$x(n)=\sum_{m=1}^{2} A_m\cos(\omega_m n+\phi_m)$$

$$=\sqrt{2}\{\cos(\frac{240\,\pi\,n}{2000}+\phi_1)+\cos(\frac{480\,\pi\,n}{2000}+\phi_2)\},$$

$$d(n)=\sum_{m=1}^{2}\{w_{I,m}^{*}x_{I,m}+w_{Q,m}^{*}x_{Q,m}\}$$

$$=0.6\,x_{I,1}(n)-0.1\,x_{Q,1}(n)+0.3\,x_{I,2}(n)-0.3\,x_{Q,2}(n). \tag{30}$$

The secondary path is modeled as $g_1=g_2=1$ $\theta_{c,1}=45°$ and $\theta_{c,2}=45°$. The simulation was carried out by setting 0.001 and 1 as the variances of measurement noise ρ_η^2. And the initial value of weights is zero. The simulation results were obtained by ensemble averaging 1000 independent runs.

1.the convergence property of FXLMF algorithm

Fig. 5. showed the summed variance convergence curve of weight error for the FXLMF algorithm that resulted from the simulation when $\mu_{Fx,1}=0.2$, $\rho_\eta^2=0.001$, and $|\triangle\theta_{c,1}|=15°$. We see that $V^2(n)$ is the dominant term during the transient state whereas $\rho^2(n)$ becomes dominant during the steady state.

Fig. 6. showed the summed variance convergence curve of weight error that resulted from the simulation when the phase estimation error $|\triangle\theta_{c,m}|$ is (1) 0°, (2) 45°, (3) 60°, (4) 75° under the same value in the steady state. It

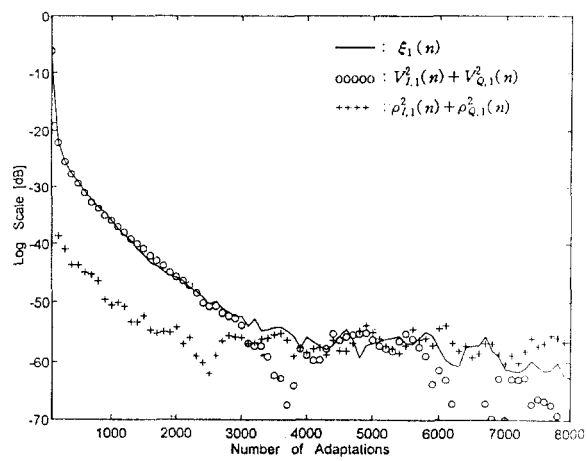

Figure 5. Learning curves for FXLMF algorithm of summed variance of weight errors when the convergence behavior are divided between $V_2(n)$ and $\rho^2(n)$

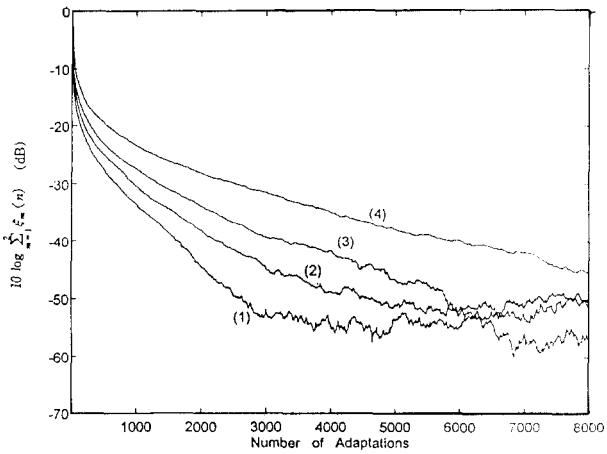

Figure 6. Learning curves for filtered-x LMF algorithm of summed variance of weight errors.($\mu_{Fx}=0.2$, $\rho_\eta^2=0.001$) (1) $|\triangle\theta_{c,m}|=0°$. (2) $|\triangle\theta_{c,m}|=45°$. (3) $|\triangle\theta_{c,m}|=60°$. (4) $|\triangle\theta_{c,m}|=75°$.

can be seen that the larger phase estimation error is, the slower the convergence speed is, and that the steady-state value is not affected by the phase estimation error $|\triangle\theta_{c,m}|$

2. the comparison of FXLMF and FXLMS

We have compared the convergence behavior of FXLMF algorithm and that of algorithm FXLMS through simulation. The convergence speed of the two algorithm were compared after setting the steady-state values equal. The convergence constants of FXLMF and FXLMS algorithm were carefully chosen so that they satisfy the conditions given in (29) for a given variance of measurement signal. To be specific, we selected 0.2 and 0.0002 for μ_{Fx} to make the steady-state values of two algorithm equal when ρ_η^2 is given as 0.001 and 1 and μ_{Sx} is 0.002.

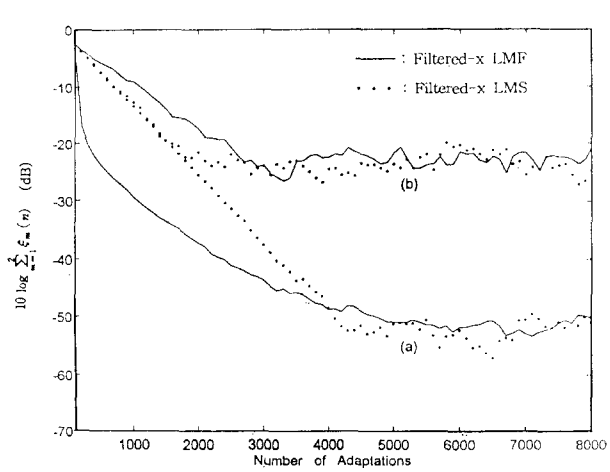

Figure 7. Comparison of the FXLMS and FXLMF algorithm learning curves of the summed variance of weight errors.
(a) $\mu_{Sx}=0.002$, $\mu_{Fx}=0.2$, $\sigma_\eta^2=0.001$, $|\Delta\theta_{c,m}|=45°$, and $V_{th}^2=0.558$.
(b) $\mu_{Sx}=0.002$, $\mu_{Fx}=0.0002$, $\sigma_\eta^2=1$, $|\Delta\theta_{c,m}|=45°$, and $V_{th}^2=558$.

In Fig. 7, the convergence behavior curves of summed variance of weight error obtained from simulation are compared with each other when the phase estimation error $|\triangle\theta_{c,m}|$ is 45°. When V_{th}^2 is sufficiently smaller than 1, we see that initially, the FXLMF algorithm converges much faster than the FXLMS algorithm but converges linearly on the logarithmic scale as the FXLMS algorithm does. When V_{th}^2 is very large, however, the FXLMF algorithm converges linearly and more slowly than the FXLMS algorithm.

V. Conclusion

The convergence result of the filtered-x LMF algorithm indicates that the effects of the parameter estimation inaccuracy on the convergence behavior of the algorithm are characterized by two distinct components: Phase estimation error and estimated gain. In particular, the convergence has been shown to be strongly affected by the accuracy of the phase response estimate. Also, it has been found that the mean square convergence behavior can differ depending on the power of Gaussian measurement noise and the size of convergence constants. Accordingly, the transient behavior can be characterized by one of the two cases: (1) initially, the Filtered-x LMF algorithm converges much faster than the FXLMS, but soon after that, it converges almost linearly on logarithmic scale like the FXLMS algorithm; (2) the FXLMF algorithm converges linearly and at a slower rate than the FXLMS. To sum up, different convergence behavior was observed depending on the variance of Gaussian measurement noise and the magnitude of convergence constant.

References

1. S. J. Elliott and P. A. Nelson, "The Active Control of Sound," *Jour. Electronics and Communication* Eng., pp. 127-136, 1990.

2. R. R. Leitch and M. O. Tokhi, "Active Noise Control Systems," *Proc. IEE*, Vol. 134, Pt. A, No. 6, pp. 525-546, 1987.

3. B. Widrow and S. D. Stearns, *Adaptive Signal Processing*: *Prentice-Hall*, 1985.

4. J. C. Burgess, "Active Adaptive Sound Control in a Duct: A Computer Simulation," *Jour. Acoust. Soc. Am.*, Vol. 70, No.

3, pp. 715-726, 1981.
5. E. Walach and B. Widrow, "The Least Mean Fourth (LMF) Adaptive Algorithm and Its Family," *IEEE Trans. on Information Theory*, Vol. 30, No. 2, pp. 275-283, March 1984.
6. S. J. Elliott, I. M. Stothers and P. A. Nelson, "A Multiple Error LMS Algorithm and Its Application to the Active Control of Sound and Vibration," *IEEE Trans. on Acoustics, Speech and Signal Processing*, Vol. 35, No. 10, pp. 1423-1434, October 1987.
7. K. S. Lee, J. C Lee, D. H. Youn and I. W. Cha, "Convergence Analysis of the Filtered-x LMS Active Noise Canceller for a Sinusoidal Input," *Fifth Western Pacific Regional Acoustic Conference*, Vol. 2, pp. 873-878, August 23-25 1994.
8. K. S. Lee, J. C. Lee and D. H. Youn, "On the Convergence Behavior of the Filtered-x LMS Active Noise Canceler," *IEEE International Workshop on Intelligent Signal Processing and Communication Systems, October* 5-7, 1994.
9. J. S. Bendat, *Nonlinear System Analysis and Identification from Random Data : Jhon Wiley & Sons*, 1990.

▲Kang Seung Lee

Kang Seung Lee received the B.S., M.S. and Ph.D. degreed in electronic engineering from Yonsei Univ., Seoul, Korea, in 1985, 1991 and 1995, respectively.

He was with the Korea Electric Power Corporation from 1995 to 1996. Since 1996, he has been with the Department of Computer Engineering, Dongeui University.

His research interests include digital signal processing and information processing.

▲Dae H. Youn

Dae H. Youn was bone in Chungju City, Korea, in 1951. He received the B.S. degree in electronic engineering from Yonsei University, Seoul, Korea, in 1977, and the M.S and Ph.D. degrees from Kansas State University, Manhattan, KS, in 1979 and 1982, respectively.

From 1979 to 1982, he served as a Reserch Associate at Kansas State University. From 1982 to 1985, he served as an Assistant Professor in the Department of Electrical and Computer Engineering, University of Iowa, Iowa city. Since 1985, he has been with the Department of Electronic Engineering, Yonsei University. His reserch interests include adaptive digital signal processing, spectrum estimation, image data compression, and speech signal processing.

He is a member of IEEE(the Institute of Electrical and Electronics Engineers), the Korea Institute of Telematics and Electronics, the Korean Institute of Communication Sciences, and an executive board of Acoustical Society of Korea. And he is a vice president of AES(Audio Engineering Society) Korea Section.